JOURNAL OF MATERIALS SCIENCE **39** (2004) 3129–3135

Ferroelectric phase transition in sol-gel derived Bi-doped PLZT ceramics

S. DUTTA*, R. N. P. CHOUDHARY*,†, P. K. SINHA§
*Department of Physics & Meteorology, and §Department of Aerospace Engineering, Indian Institute of Technology, Kharagpur-721302, India
E-mail: crnpfl@phy.iitkgp.ernet.in

Polycrystalline samples of Bi-modified PLZT, $[Pb_{0.92}(La_{1-z}Bi_z)_{0.08}][Zr_{0.60}Ti_{0.40}]_{0.98}O_3$ (abbreviated as PLBZT) for $z = 0.0$, 0.3, 0.6, 0.9 and 1 were prepared through a metal-alkoxide/sol-gel route. Preliminary X-ray diffraction study of the compounds confirmed the formation of single-phase tetragonal compounds. Scanning electron-microscopic (SEM) study of pellet samples of PLBZT shows uniform distribution of grains (spherical) throughout the sample surfaces. Detailed studies of dielectric parameters (dielectric constant, tangent loss) of PLBZT as a function of temperature (30 to 450°C) at 10 kHz reveal that the compounds have diffuse phase transitions. Large variation (first increase and then decrease) in dielectric constant and shift of transition temperature towards higher temperature side with increasing Bi concentration was also observed in PLBZT. The nature of variation of dc resistivity shows that the titled compounds have negative temperature coefficient of resistance (NTCR). Pyroelectric coefficient of the PLBZT compound ($z = 0.0$ to 1.0) increases with increase of Bi content in PLZT. The transition temperature obtained in this study is very much consistent with that obtained from our dielectric studies. Piezoelectric d_{33} coefficient of the compound at 100 Hz was found to be 385, 272, 301, 248 and 291 pc/N for $z = 0.0$, 0.3, 0.6, 0.9 and 1 respectively.

1. Introduction

Lead zirconate titanate $Pb(ZrTi)O_3$ (PZT); member of perovskite family, is a complex system of ferroelectric $PbTiO_3$ (PT, $T_c = 490$°C) and antiferroelectric $PbZrO_3$ (PZ, $T_c = 230$°C) in different Zr/Ti ratio. It has been found that substitution of some suitable ions (called modifier) at the Pb-site for different Zr/Ti ratio (i.e., 35/65 to 65/35) generally creates distortion and modification in crystal structure and physical properties. However, substitution of La^{3+} at the Pb-site of PZT (called as PLZT) drastically change piezoelectric, pyroelectric and optoelectronic properties of the materials useful for many devices such as computer memory and display devices, pyroelectric and gas sensors, electro-optical modulators, hydrophones, transducers, sonar projector, ferroelectric cathode with high current density, nonvolatile random access memory (NVRAM) and dynamic random access memory (DRAM) etc. [1–4]. The phase diagram of PT-PZ-La_2O_3 shows that $(PbLa)(ZrTi)O_3$ system with 8–10% La concentration (by atomic weight), being in the near vicinity of morphotropic phase boundary (MPB), has been reported as a good quadratic modular and piezoelectric device material [5]. Most of the physical properties of PLZT can also be improved by using suitable processing techniques. Of all the synthesis methods currently known to us, the sol-gel technique has been found to be most suitable for fabrication of fine and homogeneous PZT/PLZT powders [6]. Substitutions of single and double ion (alkali, rare earth ions) at the Pb-sites [7–11], for different Zr/Ti ratios (65:35, 60:40 and 53:47 near MPB have provided very promising materials for many devices. An extensive literature survey on PZT/PLZT showed that PLZT with Zr/Ti ratio of 60:40 and trivalent ion substitution at the La-site have not much been studied so far. This has attracted us to carry out detailed studies of structural, microstructural, dielectric, electrical, piezo and pyroelectric properties of sol-gel prepared Bi-modified PLZT compounds i.e., $[Pb_{0.92}(La_{1-z}Bi_z)_{0.08}][Zr_{0.60}Ti_{0.40}]_{0.98}O_3$ (abbreviated as PLBZT) for $z = 0.0$, 0.3, 0.6, 0.9 and 1 for better understanding of the nature of phase transitions and suitability of device applications.

2. Experimental

The polycrystalline samples of $[Pb_{0.92}(La_{1-z}Bi_z)_{0.08}][Zr_{0.60}Ti_{0.40}]_{0.98}O_3$ ($z = 0.0$, 0.3, 0.6, 0.9, 1) were prepared by a modified sol-gel technique [13] using lead acetate trihydrate $Pb(CH_3COO)_2 \cdot 3H_2O$ (99.5%, M/s Merck, India), lanthanum acetate hydrate $(CH_3COO)_3La{\cdot}xH_2O$ (99.9%, M/s. Aldrich, USA),

†Author to whom all correspondence should be addressed.

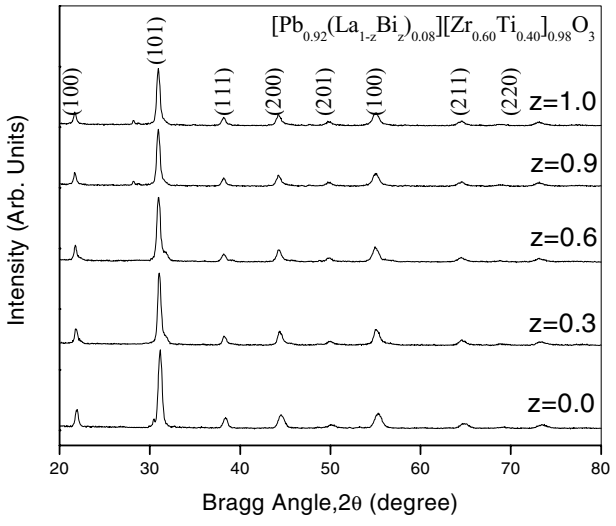

Figure 1 Room temperature XRD pattern of PLBZT.

bismuth acetate (99.9%, M/s. Aldrich, USA), zirconium isopropoxide $Zr(OC_3H_7)_4$ (70 wt% solution in 1-propanol, M/s. Fluka, Switzerland) and titanium isopropoxide $Ti(OCH(CH_3)_2)_4$ (>97% Ti, M/s. Merck, Germany). Glacial acetic acid and distilled water were used as solvents. First of all, the above acetates were dissolved separately in acetic acid in the ratio of 2 gm of salt in 1 ml acid, and these were heated at 110°C for half-an-hour to remove the water content, and then cooled down to 80°C. The above three solutions were mixed in a beaker and stirred. During stirring of the mixture, zirconium propoxide followed by titanium iso-propoxide were added to it. A small amount of distilled water was added to get a final sol after the completion of initial reactions. The sol was kept at 80°C in a constant temperature oven for 8 h to get a clear transparent gel. The gel was then dried at 120°C for 24 h, and then a light-black powder was obtained by grinding the dried gel. The oven-dried powders of PLBZT were calcined at 900°C for 7 h. The calcined powders (light yellowish) were cold pressed into pellets under a pressure of 6×10^7 kg/m^2. The pellets were then sintered at 1250°C for 24 h. In order to prevent Pb/PbO loss and to maintain the stoichiometry of the compounds during sintering at high temperature, an equilibrium PbO vapour pressure was established with $PbZrO_3$ as setter by placing everything in a covered platinum crucible. The density of the pellets obtained using Archimedes' method was found to be ~97% of their theoretical density. The formation of the desired compounds was checked by preliminary structural analysis using X-ray diffraction (XRD) pattern recorded on calcined powder in a wide range of Bragg angles, 2θ ($20^\circ \leq 2\theta \leq 80^\circ$) at room temperature with an X-ray diffractometer Philips PW1710, Holland by Cu K_α radiation ($\lambda = 1.542$Å). The crystallite size (P) of the material was calculated from the broadening of XRD profiles using Scherrer's equation [14]: $P_{hkl} = (0.89\lambda)/(\beta_{1/2}\cos\theta_{hkl})$ where $\beta_{1/2}$ is peak width at half intensity and θ is Bragg angle. The broadening due to mechanical strain, instrumental and other means has been ignored since powder samples were used. The surface morphology/grain distribution of the pellet surface was studied with Jeol JSM-5800 scanning electron microscope (SEM). For dielectric and electrical measurements a fine silver paste was applied on the flat, polished surfaces of the sintered pellets to act as an electrode. It was then dried at 150°C and cooled to room temperature to overcome the effect of moistures, if any.

The dielectric constant (ε) and loss tangent ($\tan\delta$) of the samples were obtained as a function of frequency (10^3 to 10^6 Hz) at different temperatures (room temperature-450°C) using a HIOKI 3532 LCR Hitester and a laboratory-made sample holder, which compensate stray capacitance.

The dc electrical conductivity/resistivity was measured as a function of temperature (room temperature to 450°C) at constant electric field (60 V/cm) with the help of a KEITHLEY-617 programmable electrometer and a laboratory-made experimental set up. Piezoelectric coefficient d_{33} was measured using Piezo-Meter (PM35 Take-Control, UK) at 100 Hz (pressure 1 Newton) and room temperature. Pyroelelectric material forms a capacitive element, in which the capacitance varies with temperature and capacitor deliver a current I such that $I \propto A\,\mathrm{d}T/\mathrm{d}t$ or $I = P^{\mathrm{T}}A\,(\mathrm{d}T/\mathrm{d}t)$, where P^{T} is the pyroelectric coefficient, A is the electrode area and $\mathrm{d}T/\mathrm{d}t$ is the rate of change of temperature. $\mathrm{d}T/\mathrm{d}t$ is

TABLE I Comparison of observed [o] and calculated [c] d-values of some diffraction lines of of $[Pb_{0.92}(La_{1-z}Bi_z)_{0.08}][Zr_{0.60}Ti_{0.40}]_{0.98}O_3$ ceramics at 30°C with relative intensity in parenthesis

h k l	$z = 0.0$	$z = 0.3$	$z = 0.6$	$z = 0.9$	$z = 1.0$
1 0 0	(o) 4.0042 (22)	4.0131 (28)	4.0676 (28)	4.0676 (25)	4.0676 (14)
	(c) 4.0042	4.0131	4.0676	4.0676	4.0668
1 0 1	(o) 2.8356 (100)	2.8400 (100)	2.8847 (100)	2.8892 (100)	2.8892 (100)
	(c) 2.8356	2.8396	2.8847	2.8892	2.8897
1 1 1	(o) 2.3151 (20)	2.3180 (17)	2.3530 (17)	2.3559 (15)	2.3559 (19)
	(c) 2.3141	2.3180	2.3530	2.3555	2.3556
2 0 0	(o) 2.0039 (24)	2.0060 (20)	2.0338 (20)	2.0338 (17)	2.0338 (18)
	(c) 2.0021	2.0066	2.0338	2.0338	2.0334
2 0 1	(o) 1.7923 (13)	1.7956 (10)	1.8224 (11)	1.8224 (9)	1.8224 (8)
	(c) 1.7918	1.7952	1.8212	1.8224	1.8223
2 1 1	(o) 1.6367 (30)	1.6380 (24)	1.6626 (24)	1.6626 (19)	1.6626 (23)
	(c) 1.6355	1.6387	1.6622	1.6631	1.6629
2 2 0	(o) 1.4154 (14)	1.4173 (10)	1.4387 (10)	1.4377 (10)	1.4377 (10)
	(c) 1.4157	1.4189	1.4381	1.4381	1.4378

TABLE II Lattice parameters (in Å), unit cell volume V (in Å^3), average crystallites size P (nm) and density d (gm/cc) of $[Pb_{0.92}(La_{1-z}Bi_z)_{0.08}][Zr_{0.60}Ti_{0.40}]_{0.98}O_3$ for different Bi concentrations (z). The estimated standard deviation of lattice parameters is given in parenthesis

	Tetragonal phase					
Compositions z	a	c	c/a	V	P	d
0.0	4.0042 (9)	4.0162 (6)	1.0030	64.40	11.01	7.33
0.3	4.0131 (8)	4.0183 (8)	1.0013	64.72	12.61	7.72
0.6	4.0676 (6)	4.0917 (6)	1.0059	67.70	11.21	7.86
0.9	4.0676 (3)	4.1047 (3)	1.0091	67.91	11.46	7.67
1.0	4.0668 (5)	4.1067 (5)	1.0098	67.92	11.51	7.42

maintained constant (2°C/min) over a wide temperature range. Measurement of pyroelectric current (I) has been done by dynamic method [15]. The temperature dependence of pyroelectric coefficient of the samples was obtained by measuring pyroelectric current using a laboratory-fabricated heating arrangement and a digital picoammeter (M/S Scientific Equipment Roorkee, Model DPA-111). For the piezo and pyroelectric measurements, the samples were poled at 100°C in a silicon oil bath under a dc field of 10 kV/cm for 24 h using APLAB high voltage dc power supply (model 7342P).

3. Results and discussion

In Fig. 1 we have compared the XRD pattern (recorded at room temperature) of all the Bi-modified PLZT samples. The sharp and single diffraction peaks of PLBZT with Bi = 0.0, 0.3, 0.6, 0.9 and 1.0 confirmed homogeneity and crystallization of the samples. All the reflection peaks were indexed and lattice parameters of PLBZT were determined in tetragonal, orthorhombic and cubic crystal system. Finally a particular unit cell in tetragonal system was selected for which $\sum \Delta d = \sum(d_{obs} - d_{cal})$ was found to be minimum. Table I shows

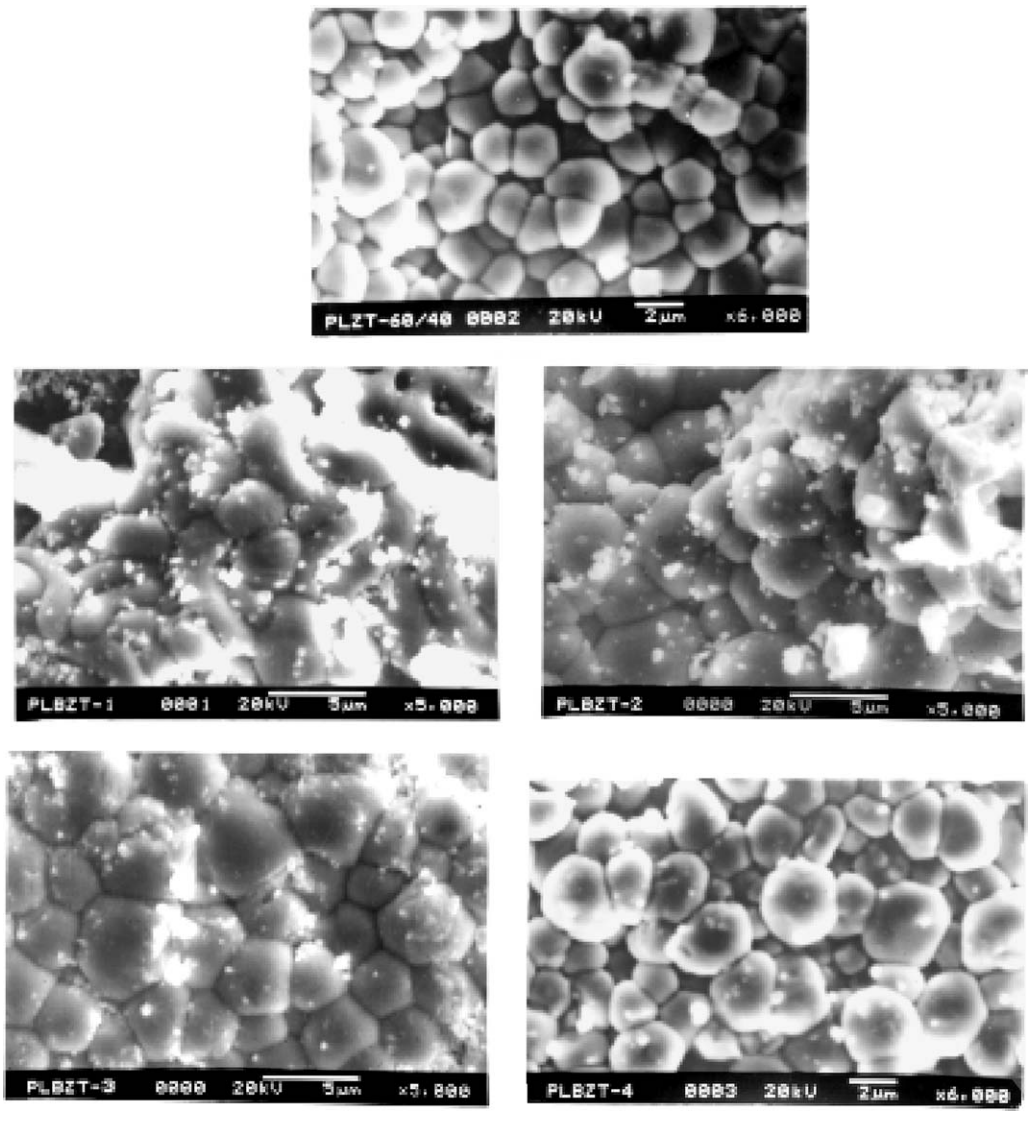

Figure 2 Scanning electron micrographs of PLBZT samples.

a good agreement between the observed and calculated *d*-values, which suggests the correctness of the selection of the crystal system and unit cell parameters. The selected lattice parameters were refined using the least-squares refinement method of the computer program package of Powd Mult [16]. It is observed that the unit cell volume is systematically increasing with the increase of Bi content this is because of the larger ionic size of Bi (1.56 Å) compared to La (1.22 Å). The lattice parameters and the measured density of PLBZT are tabulated in Table II.

The scanning electron micrograph (SEM) of the PLBZT samples (Fig. 2) indicates that the grains are nearly spherical and uniformly distributed throughout its surface. The tiny small grains with no such voids confirm high density of the ceramic samples. The grain size calculated from the SEM for $z = 0.0$, 0.3, 0.6, 0.9 and 1.0 are 989, 973, 967, 952 and 865 nm respectively.

Fig. 3 shows the variation of dielectric constant ε and dielectric loss tanδ as a function of frequency at room temperature. It was found that ε is almost constant with increasing frequency, which is observed in all the PZT/PLZT. The value of tanδ in the low frequency region (<100 kHz) first increases with the increasing frequency and becomes almost constant. The tangent loss of the pellet samples is mostly due to the scattering mechanism [5]. It was found that the room temperature value of dielectric constant ε is maximum for $z = 0.6$ afterwards it started to decrease.

Fig. 4 shows the temperature dependence of ε and tanδ for different Bi concentration (z) at 10 kHz. Similar

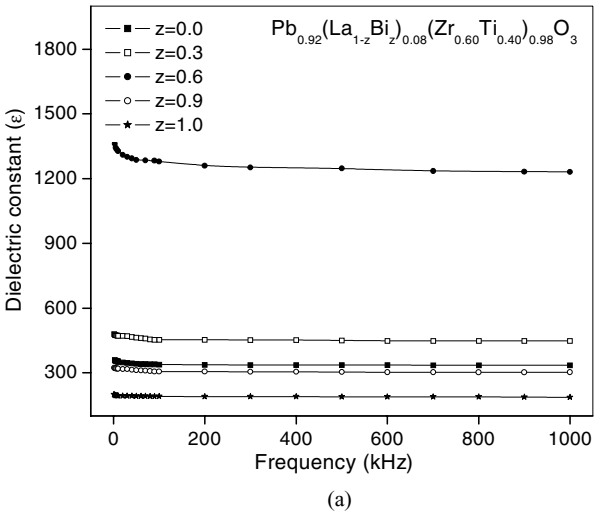

(a)

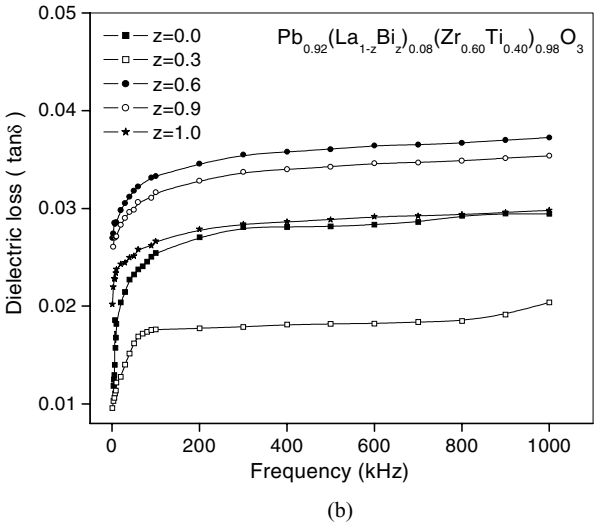

(b)

Figure 3 Variation of dielectric constant (ε) (a) and tangent loss (tan δ) and (b) of PLBZT samples with frequency at room temperature.

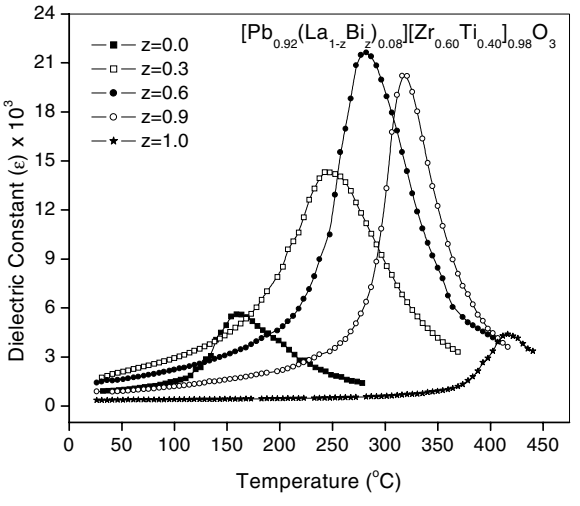

(a)

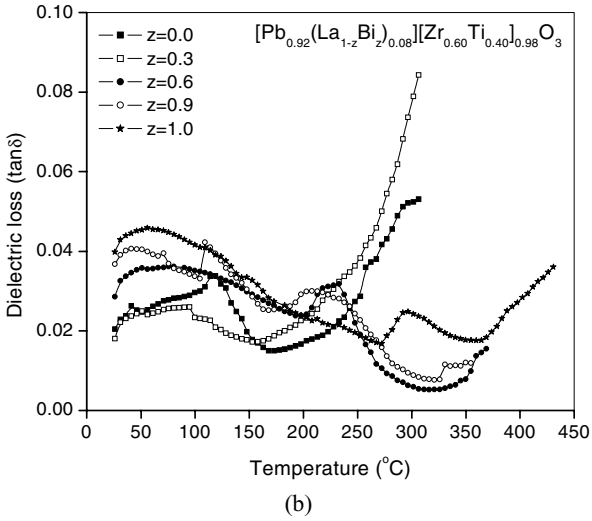

(b)

Figure 4 Variation of dielectric constant (ε) (a) and dielectric loss (tan δ) and (b) of PLBZT as a function of temperature at 10 kHz.

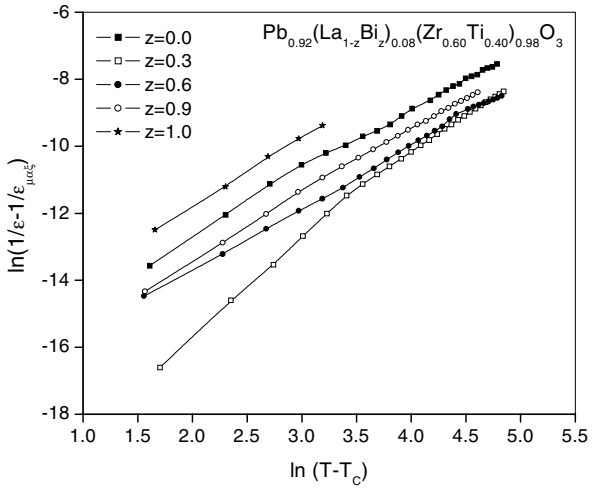

Figure 5 Variation of ln $(1/\varepsilon - 1/\varepsilon_{\max})$ of PLBZT with ln $(T - T_c)$.

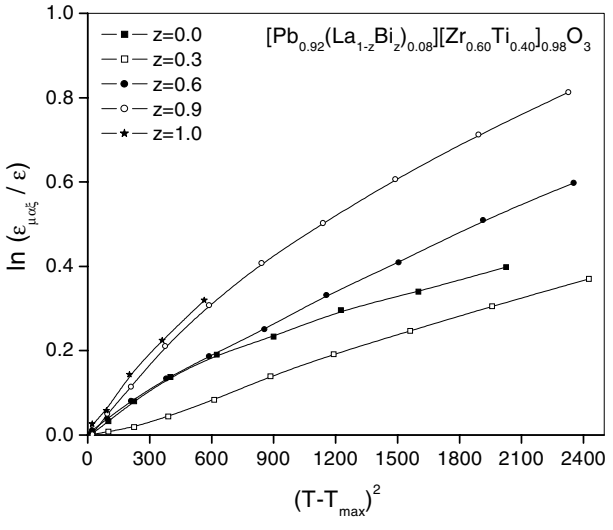

Figure 6 Variation of ln $(\varepsilon_{max}/\varepsilon)$ of PLBZT as a function of $(T - T_c)^2$.

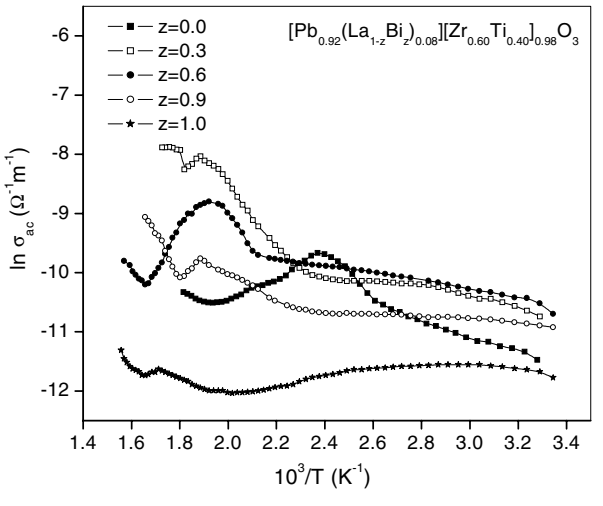

Figure 7 Variation of *ac* conductivity (lnσ) of PLBZT as a function of inverse of temperature ($10^3/T$).

to other ferroelectrics the dielectric constant of PLBZT increases gradually with rise in temperature up to its maximum value ε_{max} at a particular temperature (called T_c) and then decreases indicating the phase transition in the compounds. The dielectric peaks are found slightly broadened for $z = 0.0$–0.6 and sharp for $z = 0.9$ and 1.0. The broadened peaks indicate that the phase transition is of diffused type, which is an important characteristic of disordered and distorted perovskite materials. The broadening of the peak is attributed to the disordering in the arrangement of cations at the *A*-site and/or *B*-site leading to a microscopic heterogeneity in the composition and thus results in the distribution of different local Curie point. We also have found that the value of tanδ first increases and then decreases with increase of temperature showing a peak. At higher temperature tanδ increases faster with raise in temperature. The dielectric loss tanδ of the pellet samples may primarily be due to domain wall movement and other defects or scattering mechanism where the scattering cross-section depends on the grain size and/or the inter-grain spacing [17].

The degree of disorder of PLBZT was evaluated using an empirical expression $(1/\varepsilon - 1/\varepsilon_{max}) \propto (T - T_{max})^{\gamma}$, where γ is a measure of diffuseness of dielectric peak. The value of γ was calculated from the slope of the logarithmic plots related to the above equation (Fig. 5). It was found that the value of γ lies between 1 and 2. The higher value of γ (i.e., >1.5) confirms the existence of diffuse phase transition and disorder in PLBZT. An alternative approach is to estimate the degree of diffuseness using the relation $\ln(\varepsilon_{max}/\varepsilon) = (T - T_{max})^2/2\delta_g^2$ [18] in which δ_g is the Gaussian distribution. The variation of $\ln(\varepsilon_{max}/\varepsilon)$ with $(T - T_{max})^2$ was found to be nonlinear (Fig. 6), and hence the δ_g are evaluated at very nearer to the T_c. The calculated value of γ and δ_g of all the samples are given in Table III. Interestingly, diffuseness or diffusivity γ decreases with increasing Bi content in PLBZT. The ac conductivity of the PLBZT samples was estimated from the dielectric parameters. As the pure charge transport mechanism is the major contributor to the loss mechanisms in our system, the ac conductivity σ_{ac} was calculated using the relation $\sigma = \omega\ \varepsilon\ \varepsilon_0\ \tan\delta$ [19] in which ε_0 is the vacuum dielectric constant and ω is the angular frequency. In reality, loss tangent is due to the result of a variety of loss mechanism and separation of these varieties is a formidable task. The ac conductivity for all the samples was estimated over certain temperature range. The plot of ln σ_{ac} vs. $1/T$ (inverse absolute temperature) is shown in Fig. 7. The activation energy (E_a) of the samples was calculated in the ferroelectric and paraelectric region (near the T_c) using the relation $\sigma = \sigma_0 \exp(-E_a/k_B T)$ [20] where k_B is the Boltzmann constant. The values of activation energy E_a in the paraelectric region are comparatively lower than that of the

TABLE III Comparison of dielectric parameters, diffusivity (γ), δ_g and activation energy *Ea* (in eV) of PLBZT at 10 kHz

	Composition				
Parameters	$z = 0.0$	$z = 0.3$	$z = 0.6$	$z = 0.9$	$z = 0.0$
T_c (°C)	158	243	282	316	416
ε_{max} at T_c	5622	14321	21648	20219	4394
tan δ at T_c	0.017	0.0358	0.009	0.008	0.032
γ	1.77	1.79	1.72	1.68	1.56
δ_g	58	59	46	42	30
Ea_{ac} (ferro)	0.15	0.45	0.53	0.56	0.61
Ea_{ac} (para)	0.02	0.36	0.41	0.13	0.14
Ea_{dc} (ferro)	1.01	1.03	0.79	0.78	0.74
Ea_{dc} (para)	0.52	0.51	0.21	0.23	0.22

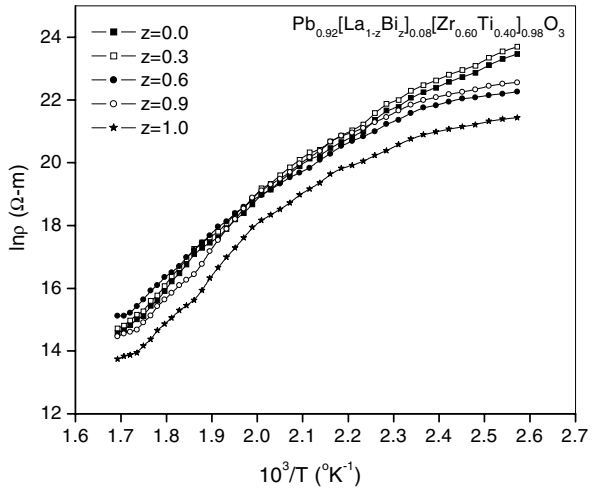

Figure 8 Variation of *dc* resistivity (lnρ) of PLBZT as a function of absolute temperature at constant electric field (50 V/cm).

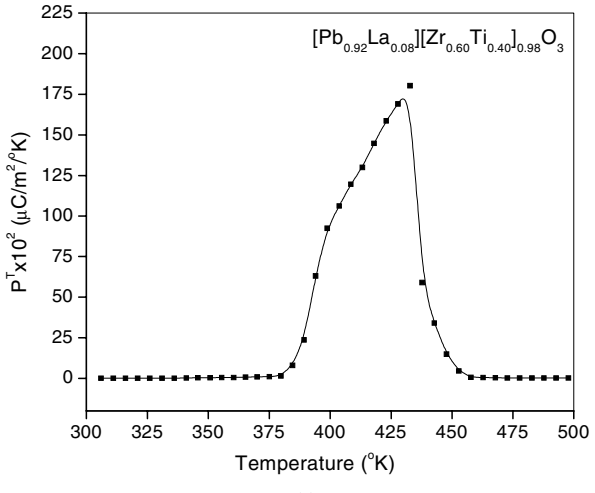

(a)

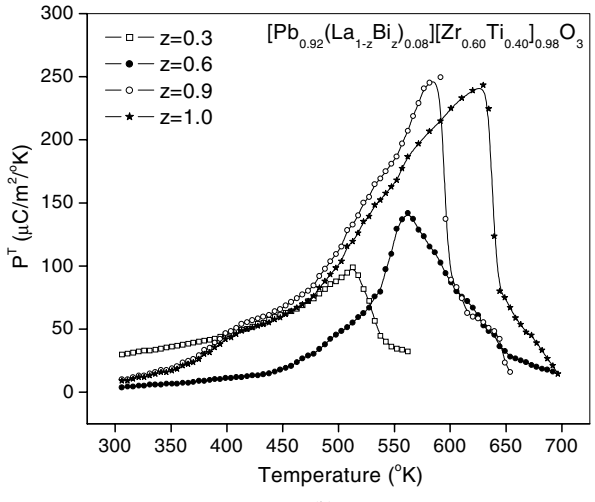

(b)

Figure 9 Variation of pyroelectric coefficient of $[Pb_{0.92}(La_{1-z})_{0.08}][Zr_{0.60}Ti_{0.40}]_{0.98}O_3$ (a) for $z = 0.0$ and (b) for $z = 0.3, 0.6, 0.9, 1$.

ferroelectric region (Table III) because in the paraelectric phase (higher temperature) less energy is required to activate the atoms.

The temperature dependence of dc resistivity of the PLBZT at constant biasing field (5 V/mm) is shown in Fig. 8. The *dc* resistivity decreases with increasing temperature for all the Bi-modified PLZTs. With the addition of thermal energy, electron could be set free from O^{2-} ions. When an electron is introduced in the sample it might be associated with cations, which results in an unstable valence state. This type of resistive behavior has also been found in many semiconductors [21], usually called NTC (negative temperature coefficient) resistors.

The piezoelectric strain coefficient (d_{33}) of the samples was found 385, 272, 301, 248 and 291 *pc/N* for $z = 0.0, 0.3, 0.6, 0.9$ and 1 respectively.

Fig. 9 shows the variation of P^T as a function of temperature. The value of P^T for PLZT is higher than the Bi-modified PLZTs. The phase transition temperature obtained from the pyroelectric measurements for different samples are in good agreement with that of the dielectric measurements.

4. Conclusion

PLBZT ceramics prepared by sol-gel technique have good homogeneity, small particle size (11 nm) and single-phase with tetragonal structure. These compounds provide many interesting features, such as the shift in transition temperature, diffuse phase transition and large variation in dielectric properties. The combination of large pyroelectric coefficients with relatively high Curie temperature makes these materials useful for pyroelectric detector applications. Piezoelectric coefficient d_{33} of the title compound was found less compared to that of PLZT.

References

1. L. H. PARKER and A. F. TASCH, *IEEE Circuits and Devices Mag* **6** (1990) 17.
2. D. STANSFIELD, "Underwater Electroacoustic Transducers" (Bath University, Bath, United Kingdom, 1991).
3. M. EINAT, D. SHUR, E. JERBY and G. ROSENMAN, *J. Appl. Phys.* **89** (2001) 548.
4. K. K. DEB, *Ferroelectrics* **82** (1988) 45.
5. M. E. LINES and A. M. GLASS, "Principles and Applications of Ferroelectrics and Related Materials" (Oxford University Press, Oxford, 1977).
6. R. OSTERTAG, G. RINN, G. TUNKER and H. SCHMIDT, *Electroceramics* Feb. (1989) 41.
7. P. ROYCHOUDHARY and S. B. DESHMUKH, *Ind. J. Pure Appl. Phys.* **17** (1981) 71.
8. S. L. FU, S. Y. CHENG and C. C. WEI, *Ferroelectrics* **67** (1986) 93.
9. R. LAL, S. C. SHARMA and R. DAYAL, *ibid.* **100** (1989) 43.
10. K. L. YADAV and R. N. P. CHOUDHARY, *ibid.* **141** (1993) 227.
11. S. R. SHANNIGRAHI, R. N. P. CHOUDHARY, H. N. ACHARYA and T. P. SINHA, *J. Phys. D. Appl. Phys.* **32** (1999) 1539.
12. K. L. YADAV and R. N. P. CHOUDHARY, *Bull. Pure Appl. Sci.* **14** (1995) 23.
13. G. YI, Z. WU and M. SAWYER, *J. Appl. Phys.* **64** (1988) 2717.
14. P. KLUG and L. E. ALEXANDER, "X-ray Diffraction Procedure of Polycrystalline and Amorphous Materials" (John Wiely and Sons, New York, 1974).
15. "Source Book of Pyroelectricity," edited by S. B. Lang (Gordon and Breach Science Publishers, London, 1974).

16. E. WU, POWD, An Interactive Powder Diffraction Data Interpration and Indexing Program, Ver 2.1, School of Physical Science Flinders University of South Australia Bedford Park S.A J042 AU.
17. B. N. ROLOV, *Sov. Phys. Solid State* **6** (1965) 1676.
18. S. MIGA and K. WOJEIK, *Ferroelectrics* **100** (1987) 167.
19. V. M. GUREVICH, "Electric conductivity of Ferroelectrics" (Israel Translation, Jerusalem-1971).
20. W. D. KINGERY, "Introduction to Ceramics" (Wiely-Intersciences, New York, 1960).
21. E. H. PUTLEY, "Semiconductors and Semimetals" (Academic Press, New York, 1970) Vol. 5, Chap. 6.

Received 5 February
and accepted 6 November 2003